EUROPEAN ORGANIZATION FOR NUCLEAR RESEARCH

CERN–SPSC–2017–XXX
SPSC-X-XXX
December 18, 2017

d-Quark Transversity

and

Proton Radius

Addendum to the COMPASS-II Proposal

The COMPASS Collaboration
and
PNPI

v3.1 19.12.2017 10:44

contact: O. Denisov/Torino, J. M. Friedrich/TUM
COMPASS spokespersons
Oleg.Denisov@cern.ch, Jan.Friedrich@cern.ch

The COMPASS Collaboration

Joined Czech group, Prague, Czech Republic
K. Augsten, M. Bodlak, M. Finger, M. Finger jr., M. Jandek, V. Jary, K. Juraskova, A. Kveton, J. Matousek, A. Nikolovova, J. Novy, M. Pesek, M. Peskova, M. Slunecka, A. Srnka, M. Sulc, J. Tomsa, M. Virius

CEA-Saclay, IRFU, Gif-sur-Yvette, France
Y. Bedfer, A. Ferrero, N. d'Hose, F. Kunne, D. Neyret, S. Platchkov, A. Vidon

Ruhr-Universität Bochum, Bochum, Germany
W. Meyer, G. Reicherz

Rheinische Friedrich-Wilhems-Universität, Bonn, Germany
M. Ball, J. Barth, R. Beck, D. Eversheim, E. Fotina, R. Joosten, B. Ketzer, F. Klein, M. Mikhasenko, J. Pretz, R. Reyes Ramos, H. Schmieden, A. Thiel, M. Wagner

Universität Freiburg, Freiburg, Germany
M. Büchele, H. Fischer, M. Gorzellik F. Herrmann, P. Jörg

Universität Mainz, Mainz, Germany
J. Giarra, D. von Harrach, E. M. Kabuß, W. Nowak, M. Ostrick, N. Pierre, J. Pochodzalla, M. B. Veit, M. Wilfert

Technische Universität München, Munich, Germany
S. Chung, C. Dreisbach, W. Dünnweber, M. A. Faessler, J. M. Friedrich, S. Gerassimov, B. Grube, S. Huber, F. Kaspar, I. Konorov, F. Krinner, S. Paul, D. Ryabchikov, J. Seyfried, D. Steffen, S. Uhl, S. Wallner

Matrivani Institute of Experimental Research & Education, Calcutta, India
S. Dasgupta, L. Dhara, A. Roy, S. Sarkara, L. Sinha

Tel Aviv University, Tel Aviv, Israel
J. Lichtenstadt

INFN, Sezione di Torino, e Università di Torino, Turin, Italy
M. G. Alexeev, A. Amoroso, F. Balestra, M. Chiosso, O. Denisov, I. Gnesi, A. Grasso, A. Ivanov, A. M. Kotzinian, R. Longo, A. Maggiora, D. Panzieri,B. Parsamyan, F. Tosello

INFN, Sezione di Trieste, e Università di Trieste, Trieste, Italy
J. Agarwala, F. Bradamante, A. Bressan, C. Chatterjee, A. Cicuttin, M. Crespo, S. Dalla Torre, S. Dasgupta, A. Kerbizi, S. Levorato, N. Makke, A. Martin, A. Moretti, G. Sbrizzai, A. Szabelski, S. Tessaro, F. Tessarotto

Japanese Group, Yamagata, Japan
N. Doshita, N. Horikawa, S. Ishimoto, T. Iwata, K. Kondo Horikawa, T. Matsuda, Y. Miyachi, G. Nukazuka, H. Suzuki

National Centre for Nuclear Research and University of Warsaw, Warsaw, Poland
W. Augustyniak, B. Badełek, K. Kurek, B. Marianski, A. Sandacz, P. Sznajder,

Warsaw University of Technology, Warsaw, Poland
R. P. Kurjata, J. Marzec, A.Rychter, K. Zaremba, M. Ziembicki

University of Aveiro, Aveiro, Portugal
C. Azevedo, F. Pereira, J. Veloso

Laboratory of Instrumentation and Experimental Particles Physics, Lisbon, Portugal
P. Bordalo, C. Franco, C. Menezes Pires A. S. Nunes, C. Quintans, S. Ramos, L. Silva, M. Stolarski

JINR, Dubna, Russia
R. Akhunzyanov, G. D. Alexeev, N. V. Anfimov, V. A. Anosov, A. Efremov, V. Frolov, O. P. Gavrichtchouk, A. Gridin, R. Gushterski, A. Guskov, Yu. Ivanshin, A. Janata, Yu. Kisselev, O. Kouznetsov, G. V. Meshcheryakov, E. Mitrofanov, N. Mitrofanov, A. Nagaytsev, A. Olshevski, D. V. Peshekhonov, A. Rybnikov, A. Samartsev, I. A. Savin, A. Selyunin, J. Smolik, P. Zavada, E. Zemlyanichkina, N. Zhuravlev

P. N. Lebedev Physical Institute of the Russian Academy of Sciences, Moscow, Russia
V. Tskhay, M. Zavertyaev

IHEP, Protvino, Russia
S. V. Donskov, G. V. Khaustov, Yu. A. Khokhlov, V. N. Kolosov, V. F. Konstantinov, Yu. V. Mikhailov, V. A. Polyakov, V. D. Samoilenko

Polytechnic University, Tomsk, Russia
V. E. Burtsev, A. G. Chumakov, G. Chursin, R. R. Dusaev, I. I. Kuznetsov, E. A. Levchenko, V. E. Lyubovitskij, S. A. Mamon, K. Sharko, B. Vasilishin

CERN, Genève, Switzerland
G. K. Mallot, O. Subrt, A.Vauth

Academia Sinica, Taipei, Taiwan
W. Chang, C. Hsieh, Y. Lian, M. Quaresma

University of Illinois, Urbana-Champaign, USA
V. Andrieux, F. Gautheron, M. Grosse Perdekamp, R. Heitz, J. H. Koivuniemi, Y. Kulinich, A. Magnon, N. Makins, M. Meyer, J. Peng, C. K. Riedl

and

Petersburg Nuclear Physics Institute of National Research Center, "Kurchatov institute", St. Petersburg, Russia
E. Maev, A. Dzyuba, G. Gavrilov, V. Golovtsov, A. Vasilyev, A. Vorobyev

Contents

Executive summary

As outlined in the proposal for the ongoing COMPASS-II programme, the research fields of hadron spectroscopy and hadron structure are closely connected since their very beginnings, leading to the establishment of Quantum Chromodynamics (QCD) of quarks and gluons as the theory of strong interactions. It explains the observed weakening of the interquark forces at short distances or large momentum transfers. QCD not only describes hard processes through perturbative expansions, but also the non-perturbative dynamics of the strong interaction, down to soft and extremely soft processes which are involved in meson spectroscopy and linked to chiral perturbation theory. Also the finite extension of the hadrons, as encoded in the nucleon form factors, is connected to their inner dynamics and thus a decisive test field for QCD.

The COMPASS-II proposal covers three important processes in that context, namely deeply-virtual Compton scattering, Drell-Yan dimuon production off a polarised target, and Primakoff reactions on nuclei giving access to soft pion-photon reactions. This programme is foreseen to be completed in the end of the year 2018, after the second year of data taking for polarised Drell-Yan processes, before the long shutdown period LS2 in 2019 and 2020.

The impressive scientific output of COMPASS and COMPASS-II and the rapid progress in the fields of our investigation make us consider various future scenarios where we could again make important contributions, further exploiting the capabilities of the M2 beam line and of an upgraded spectrometer. They are currently being collected in a Letter of Intent that is planned to be submitted within the coming months. It will contain, beyond the usage of the conventional, by now available beams, longer-term perspectives with radiofrequency-separated (kaon) beams, with a physics programme of about 10 years, and is worked out within the CERN Physics Beyond Colliders initiative.

Since the CERN Research Board has approved in the memorandum DG-Dr-RCS-2017-093 an early post-LS2 fixed-target programme and running, the COMPASS-II collaboration has decided to propose two physics cases of the future programme, as an addendum to the ongoing programme for data taking immediately after LS2.

The first programme, semi-inclusive DIS on transversely polarized deuterons, is the "missing piece" in the COMPASS data sets on transverse target spin orientations. In 2010, a dedicated run was taken on a transversely polarised proton (NH3) target, which provided pioneering and unique information on transversity and Sivers functions, underlining the importance of transverse spin in the QCD structure of the nucleon and the correctness of conjectures put forward 25 years ago. On the contrary we provided only a marginal (albeit unique) data set for the isoscalar deuteron target. The older data have been taken only for short periods in the first years of COMPASS running and with the low-aperture SMC target magnet. With one additional year of data taking, which is proposed here, the statistics can be enhanced by up to a factor 20, allowing accurate flavour separation for the new functions and measurements which will stay unique for many years to come.

The second programme, elastic muon-proton scattering, represents a new physics case for COMPASS. It was recognized recently that in the context of the currently debated "proton radius puzzle", high-energy muon-proton elastic scattering is a decisive experimental method that is complementary, in part even superior to the manifold of other proposed or ongoing experiments. With a dedicated hydrogen gas target to be contributed by the St. Petersburg group, who has developed a similar target for an experiment with electron beams at Mainz, COMPASS-II is seen to be the ideal – in fact the only – place to

realize this experiment with multi-GeV muon beams. This very appealing perspective includes the incorporation of some new equipment, and also necessitates new developments regarding the readout of the detectors, such that some testing will be indispensable.

In view of these preliminaries, the following running schedule is proposed:

2021: one year [1)] semi-inclusive DIS data taking with the transversely polarised deuteron target, and at an early stage test measurements for the proton radius measurement

2022: one year of data taking for the proton radius measurement (under the condition of a successful testing phase in 2021)

[1)] by one year of data taking we intend 150 days of data taking with 2.5×10^{13} protons delivered to the T6 target of the M2 beam line every 40.8 s. With an accelerator chain efficiency of 90% 6.1×10^{18} protons at T6 are expected.

– PHYSICS CASE –

1 Measurement of semi-inclusive deep inelastic scattering off transversely polarised deuterons

1.1 Introduction

In collinear QCD, when the transverse momentum of the partons is neglected, three parton distribution functions (PDFs) fully describe the nucleon at the twist-two level: the momentum distributions $f_1^q(x)$, the helicity distributions $g_1^q(x)$ and the transversity distributions [1] $h_1^q(x)$, where x is the Bjorken variable. On the other hand, evidence for a sizable transverse momentum of quarks was provided from the measured azimuthal asymmetries of hadrons produced in unpolarised semi-inclusive deep inelastic scattering (SIDIS) and of the lepton pairs produced in Drell-Yan (DY) processes. Taking into account a finite intrinsic transverse momentum k_T, in total eight transverse momentum dependent (TMD) distribution functions are required to fully describe the nucleon at leading twist [2, 3, 4]. Since transverse spin couples naturally to intrinsic transverse momentum, the resulting correlations are encoded in various TMD PDFs. Presently, PDFs that describe non-perturbative properties of hadrons are not calculable in QCD from first principles, but their first moments can already be computed in lattice QCD. In the SIDIS cross-section they appear convoluted with fragmentation functions (FFs) [5, 6], and can be extracted from the data.

Particularly interesting is therefore the measurement of the SIDIS cross-section when the target nucleon is transversely polarised. In this case 8 (5 in case of unpolarised lepton beam) different spin-dependent azimuthal modulations are expected, from which information on the TMD PDFs can be extracted [2)]. In this domain the HERMES and the COMPASS collaborations have performed pioneering measurements and shown beyond any possible doubt the correctness of three most interesting recent conjectures:

- The Sivers function $f_{1T}^{\perp}$: in a nucleon that is polarised transversely to its momentum the quark distribution is not left-right symmetric with respect to the plane defined by the directions of the nucleon spin and momentum. This asymmetry of the distribution function is called the Sivers effect, and the asymmetric function is known as the Sivers PDF [8].
- The Transversity function h_1: the quarks in a transversely polarised nucleon are transversely polarised. Their polarisation is described by the h_1 PDFs which a priori are different and have different properties from the helicity PDFs.
- The Collins function $H_1^{\perp}$: the hadronization of a transversely polarised quark is not left-right symmetric with respect to the plane defined by the direction of the quark momentum and the quark spin [9]. This fact has been confirmed by the e^+e^- measurements at Belle, BeBar and BES and has been exploited to measure the quark transverse polarisation in a transversely polarised nucleon, namely the quark transversity PDF.

These effects represent novel and unexpected features, and one still believes that they might explain the very large transverse spin asymmetries observed since more than 40 years in hadron-hadron scattering.

The non-zero results for the Collins and the Sivers asymmetries were obtained on proton targets. COMPASS has also measured transverse spin asymmetries using a deuteron target [10]. The accuracy of the data is definitely inferior to that of the proton data, and all the results are compatible with zero, hinting at a possible cancellation between u and

[2)] For a review of the notation we refer to the Appendix A of the memo CERN-SPSC-2009-025 SPSC-M-769, SPSLC-P-297 Add.2 [7], which for completeness is also added to this document as section 1.6.

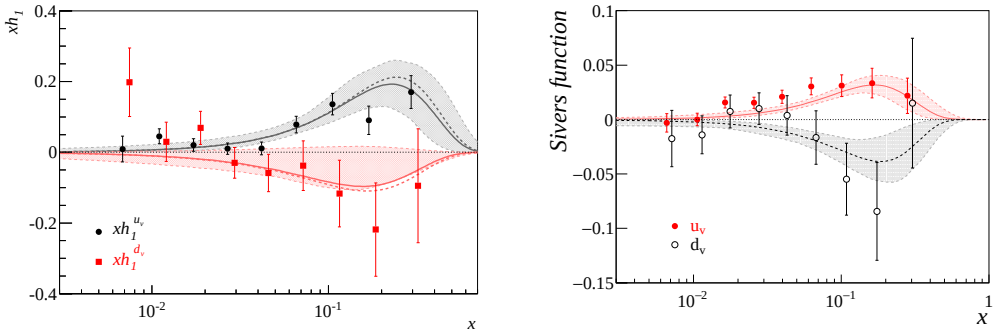

Figure 1: The transversity and Sivers PDFs extracted point-by-point using the existing COMPASS p and d data from Ref. [13, 14]. The curves are the results of fits to the COMPASS and HERMES data and, for transversity, to the Belle data. Note that the uncertainty band for the d-quark transversity would be larger if the Soffer bound was not imposed.

d quarks contributions. More recently data have been collected at much lower energy at JLab on a ^{3}He target, essentially a transversely polarised neutron target: the measured asymmetries [11, 12] are also compatible with zero, but the error bars are fairly large. The COMPASS data are still today the only SIDIS data ever taken on a transversely polarised deuteron target, they are necessary to flavour separate the PDFs, and provide constraints on the d-quark contribution.

From the present data several extractions of the transversity and of the Sivers PDFs have been performed. As an example in Fig. 1 are shown the results of the point-by-point extractions of the transversity and the Sivers PDFs using all the existing COMPASS p and d data [13, 14] compared to the extractions done using also the HERMES data [15, 16]. More recent extractions [17, 18] did not improve substantially the picture. It is immediately apparent that the accuracy of the d-quark PDFs is considerably inferior to that of the u-quark because of the bad quality of the existing d data and this is the straightforward motivation for this proposal.

We propose to perform a standard one-year (150 days) measurement, scattering the M2 muon beam at 160 GeV/c momentum on a transversely polarised deuteron target, as soon as the LS2 will be over, using the COMPASS spectrometer. The polarised target system has been reassembled at the end of the DVCS/SIDIS run, last fall, it will be used for the Drell-Yan run of 2018, and will stay installed in Hall 888 for this new measurement.

Due to the late delivery of the COMPASS polarised target magnet, this precise measurement could not be carried through in the early years of data taking when the low statistics sample was collected. It is a matter of fact, however, that the knowledge gained in the last few years thanks also to the SIDIS results has by now made the physics case very clear and strong, and we regard this measurement as necessary to complete the exploratory COMPASS programme on the transverse spin nucleon structure.

The new SIDIS asymmetry data, combined with the good precision HERMES and COMPASS proton data, and with the future high precision JLab12 data, will allow u and d distribution functions to be extracted with comparable accuracy. The future EIC will possibly supersede the existing and the proposed measurements, but the new COMPASS contribution will stay there for several years.

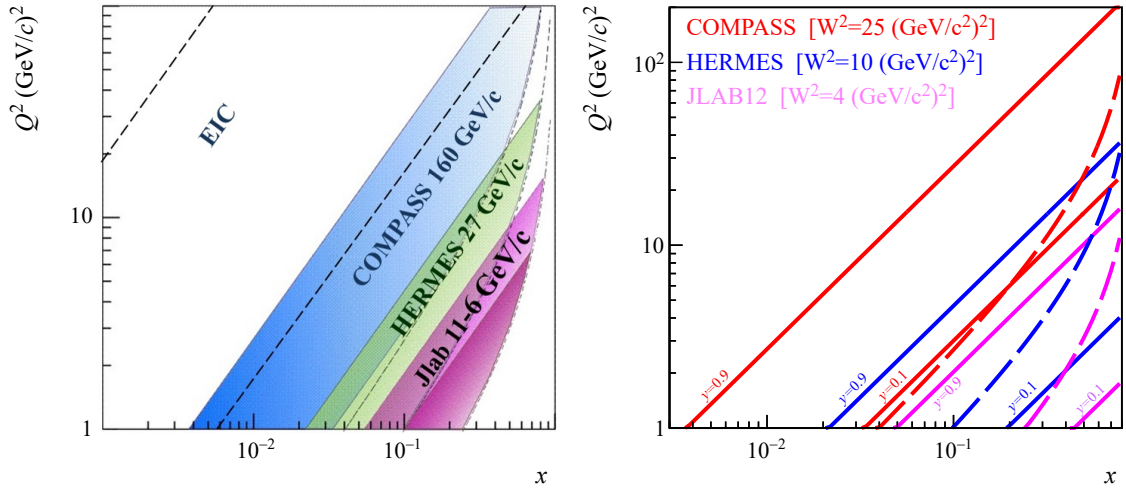

Figure 2: The $x - Q^2$ scatter plot for SIDIS experiments HERMES, COMPASS and JLab12. Left: also indicated with dash lines are the ($\sqrt{s}$ = 140 GeV , $y = 0.9$) and ($\sqrt{s} = 40$ GeV, $y = 0.1$) borders for a future EIC. Only the kinematic ranges are drawn, independently of the luminosity and of the years needed to perform the measurements. Right: the full lines indicate the $y = 0.1$ and $y = 0.9$ boundaries for the three experiments, the dashed lines the corresponding W^2 values.

1.2 The case for muon scattering on transversely polarised deuterons

High energy muon scattering on transversely polarised deuterons will provide in a standard 150 days run a wealth of data and complement the data sample collected in 2007 and 2010 on transversely polarised protons.

The new data will provide large Q^2 results in the x-range covered by JLab12, which is very important to evaluate the size of the Q^2 evolution, and will provide lower-x data (down to $x = 0.003$) which are essential both to perform the integrals necessary to evaluate the tensor charges and to estimate the TMD PDFs of the sea quarks. The phase space covered by the different experiments is shown in Fig. 2. Clearly the experiment we propose is unique and complementary to the JLab12 experiments. In the longer term the planned Electron Ion Collider (EIC) [?] has the potential to carry on a very good programme, but its start is not yet well defined in time, and colliding polarised deuterons is not in the core program: a deuteron measurement at CERN has a considerable chance of staying as an important and unique result for a couple of decades.

The case for the Collins asymmetry will be detailed in the next section. Here we will summarize some of the other measurements which will be performed in parallel using the new deuteron data. Very much as for the Collins asymmetry, all the target transverse spin asymmetries (TSA) are expected to be measured with a statistical uncertainty equal to 0.62 times the statistical uncertainties of the corresponding asymmetries measured in the 2010 proton run which we use as a reference.

1.2.1 The two hadron asymmetries

The transverse polarisation of a fragmenting quark can also be assessed from the modulation of the distribution of the azimuthal angle of the plane containing two oppositely charged hadrons of the jet. This di-hadron asymmetry can be expressed as the product of the quark transversity distribution and a chiral-odd di-hadron FF, $H_1^{\sphericalangle}$, which survives af-

ter integration over the two hadron momenta, and thus can be analyzed in the framework of collinear factorization. The high energy of the beam and the large acceptance of the COMPASS spectrometer have allowed us to collect in 2010 a large sample of (oppositely charged) hadron pairs. From the measured di-hadron asymmetries and from corresponding data of the Belle experiment fairly precise estimates of the u-quark transversity distribution could be obtained [13, 19], while the d-quark extraction has considerably larger uncertainties, very much as for the Collins asymmetry case. Also, a unique and original comparison between the single-hadron Collins asymmetry and the di-hadron asymmetry could be performed [20, 21]. The conclusion of this investigation was that both the single hadron and the di-hadron transverse-spin dependent fragmentation functions are driven by the same elementary mechanism, which is very well described in the $^3P_0$ recursive string fragmentation model [22, 23]. A corresponding analysis with the deuteron data was not possible because of the particularly small statistics of the two hadron data sample due to the use of the small acceptance PT magnet used in the first three years of COMPASS running. The new deuteron data therefore will provide more information both on the transversity PDFs and on the di-hadron FF.

1.2.2 The Sivers function

As underlined in Ref. [14], and clear from Fig. 1, the d_v Sivers function is poorly determined from the present data, in spite of the fact that it should be constrained by the PID of the final state hadrons. Moreover, the Sivers asymmetry exhibits strong kinematic dependencies [**?**] which are not easy to be explained. Keeping in mind that the COMPASS kinematic coverage lays between JLAB (6 and 12 GeV) and a future EIC, the proposed COMPASS measurements will stay as a unique bridge between the two. Using all the three measurements, one can have the opportunity to understand the confined motions of unpolarised quarks inside of a transversely polarised nucleon. For these reasons, the new deuteron data are badly needed and will allow to measure the Sivers asymmetries with a statistical error 0.62 times smaller than that of the existing COMPASS proton data, very much as in the Collins case.

The assessment of a non-zero Sivers function for the quarks and its possible connection with the orbital angular momentum have stimulated a great interest in a possible non-vanishing Sivers function for the gluon and considerable further theoretical work (see f.i. [**?**]). A recent analysis of proton-proton data at RHIC has not evidenced a signal [**?**]. However, an analysis of all the COMPASS data has provided some indication that the gluon Sivers function might be different from zero [24]. The accuracy of the existing deuteron data is worse by a factor of about 2 than that of the proton data and the new data would allow to have a measurement of the gluon Sivers asymmetry with a statistical uncertainty of 0.05, to be compared with the present uncertainty of 0.08.

In a similar analysis the Sivers asymmetry for the J/Ψ has also been determined, which in some models is related to the gluon Sivers asymmetry [25]. That analysis can also be repeated and improved with the new deuteron data.

1.2.3 The g_2 structure function

In the naive parton model g_2 is expected to be zero, thus its measurement provides information on the quark-gluon interaction. In COMPASS we have started an analysis to extract g_2 from the 2010 proton data, which will be repeated with the new deuteron data. After standard cuts we have slightly more than 10^8 DIS events. Compared to previous measurements done by SLAC on proton and deuteron (E142, E143, E154 and E155) and

by HERMES (proton), COMPASS explores a larger kinematic range accessing also the essentially unknown low-x region ($0.003 < x < 0.05$). So far the efforts are concentrated on the extraction of the g_2-related inclusive asymmetry, $A_T^{cos\phi_S}$ (where the angle ϕ_S is defined in the $\gamma^* N$-system as the azimuthal angle between the lepton scattering plane and the target spin direction) and the virtual photon-absorption asymmetry A_2. The estimated statistical uncertainties of the $A_T^{cos\phi_S}$ asymmetry in the different kinematic bins are comparable with the corresponding uncertainties of the Sivers asymmetries extracted from the 2010 proton SIDIS sample.

It is interesting to note that, from constraints imposed by Lorentz invariance relations, g_2 is expected to be linked to the first k_T-moment of the g_{1T} TMD PDF which is being accessed in SIDIS through the measurement of $A_{LT}^{cos(\phi_h - \phi_S)}$ asymmetry. This is yet another effect we plan to address with the deuteron measurement and another piece of information that can be acquired.

1.2.4 Other SIDIS measurements

COMPASS has performed a multidimensional extraction of the whole set of target transverse spin dependent azimuthal asymmetries using the proton data collected in 2010 [26]. Various multi-differential configurations have been tested exploring the $x - Q^2 - z - p_T$ phase-space. Very interesting correlations have been noticed in particular for the Sivers function. This analysis was not possible with the existing deuteron data, and will be done with the new data.

Finally, COMPASS has recently extracted the "p_T-weighted" Sivers asymmetries from the 2010 proton data [**?**]. These results allow to directly derive the first moment of the Sivers function [**?**]. Also this analysis which could not be done with the existing deuteron data, will be performed on the new data set.

1.2.5 Exclusive vector meson production

In exclusive vector meson production COMPASS has produced several interesting results. In a first paper [27] we published the transverse target spin azimuthal asymmetry $A_{UT}^{\sin(\phi-\phi_S)}$ in hard exclusive production of ρ^0 mesons which we measured both on transversely polarised protons and deuterons. The measured asymmetry is sensitive to the nucleon helicity-flip generalized parton distributions E_q, which are related to the orbital angular momentum of quarks in the nucleon. A second publication [28] used the high statistics proton data collected in 2010, and presented results for all 8 possible transverse target spin asymmetries. In particular a specific combination of two of these asymmetries indicates a signal from the so called "transversity GPD" (i.e. GPD with the helicity flip of exchanged quark). Concerning deuterons, only the results on the $A_{UT}^{\sin(\phi-\phi_S)}$ asymmetry are published [27], due to the poor statistics of the existing deuteron COMPASS data. Given the expected small contribution of the gluons and sea quarks [**?**] very much as for the SIDIS case, a combined analysis of both proton and deuteron data is necessary to disentangle the u and d quark GPDs, thus new accurate deuteron data are essential to carry through this analysis. In parallel, the exclusive production of ω will also be measured. The cross-section is smaller by about a factor 10 than for ρ^0 mesons and the detection of the two photons further reduces the ω event sample with respect to the ρ^0, but a combined analysis of ρ^0 and ω mesons provide strong constrains in disentangling the u and d quark contributions.

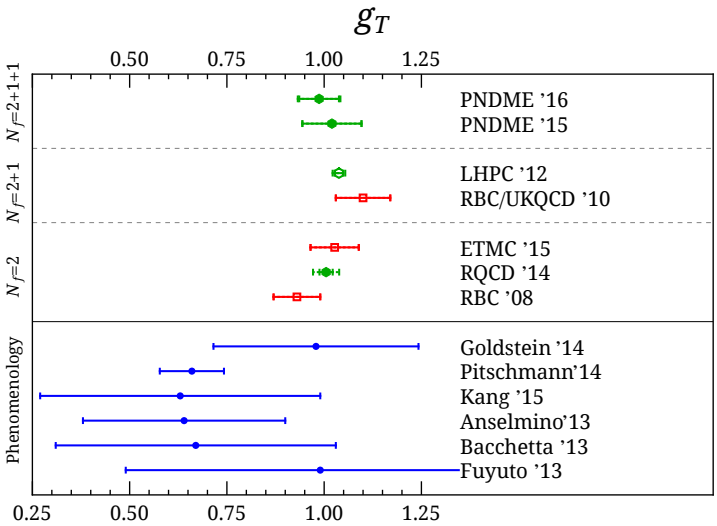

Figure 3: A summary plot showing the current estimates of g_T^{u-d} from Ref. [30]. Green and blue points come from lattice calculations while the black points are from phenomenological extractions from the data.

1.3 The case for transversity

In this section the impact of the new deuteron measurement for the Collins asymmetry and for the extraction of transversity for the u and d quarks will be detailed. The measurement of the transversity distributions, which are defined in terms of the nucleon matrix element of the quark tensor current, is particularly important because it provides access to the tensor charges δq, which are given by the integral

$$\delta q(Q^2) = \int_0^1 dx [h_1^q(x, Q^2) - h_1^{\bar{q}}(x, Q^2)] \tag{1}$$

In a non-relativistic quark model, h_1^q is equal to g_1^q, and δq is equal to the valence quark contribution to the nucleon spin. The difference between h_1^q and g_1^q provides important constraints to any model of the nucleon. Knowing the quark tensor charges one can construct the isovector nucleon tensor charge $g_T = \delta u - \delta d$, a fundamental property of the nucleon which, together with the vector and axial charge, characterizes the nucleon as a whole. Since many years the tensor charge is being calculated with steadily increasing accuracy by lattice QCD [29]. More recently, its connection with possible novel tensor interactions at the TeV scale in neutron and nuclear β-decays and its possible contribution to the neutron electric dipole moment (EDM) have also been investigated [30], and possible constraints on new physics beyond the standard model have also been derived [31].

The present knowledge on g_T is well summarized in Fig. 3, from Ref. [30]. The huge difference between the accuracy of the extractions from the existing data and from the QCD lattice simulations is striking and more experimental data are needed. When evaluating the tensor charge from the transversity data h_1^u and h_1^d have the same weight, so

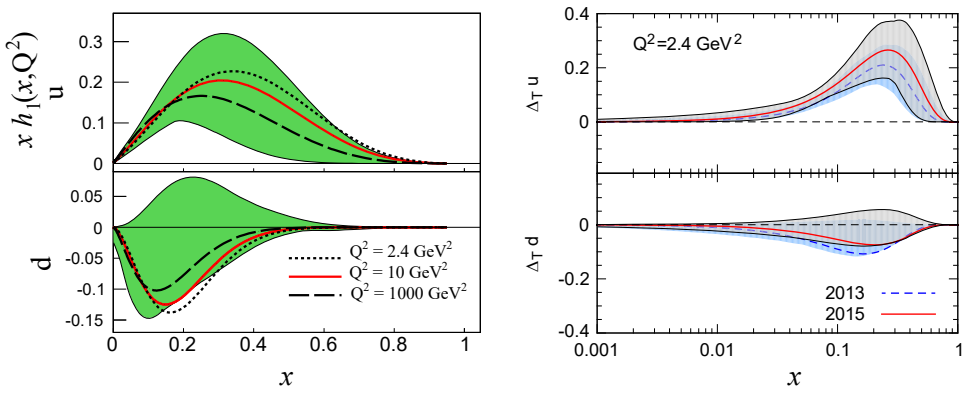

Figure 4: The u and d quark transversity PDFs from recent global fits. The plots are from Ref. [17] (left) and from Ref. [18] (right).

they must be known with a comparable accuracy. In SIDIS off protons, because of the opposite sign of the favored and unfavored Collins FF, the Collins asymmetries of positive and negative pions depend almost on the same linear combination of h_1^u and h_1^d, with weights 4 and 1, so basically to first approximation it is impossible to precisely extract the d-quark transversity without deuteron (or neutron) data. This means that most of the present uncertainty in the tensor charge are due to the poor accuracy of the deuteron data, and that remeasuring the deuteron is a priority issue.

In Fig. 1 we have shown the point-by-point extraction of the u- and d- transversity PDF of Ref. [13] which clearly indicates the inadequacy of the existing data to extract h_1^d. This is the case even for the most recent extractions, which utilize all existing SIDIS data (from COMPASS, HERMES and JLab) and the constraints given by the Soffer bound. Two very recent extractions, from Ref. [17] and from Ref. [18], are shown in Fig. 4, and both give the same message, that new accurate SIDIS data on the deuteron are necessary to improve on the d-quark transversity.

In the near future the only planned and approved experiments will run at JLab12 [32, 33], with both proton and neutron targets, and very good statistics, but only in the region $x > 0.05$ and at relatively small Q^2. The main objective of our proposal is to measure from $x = 0.3$ down to 0.003 and at larger Q^2, improving the accuracy of the extraction of h_1^d and improving also the precision of h_1^u as will be shown in the next sections.

1.3.1 Present COMPASS data and extrapolated errors

The transversity PDF is chiral-odd and thus not directly observable in inclusive deep inelastic lepton-nucleon scattering. In 1993 Collins suggested [9] that it could be measured in SIDIS processes, where it appears coupled with another chiral-odd function, which by now is known as "Collins fragmentation function" $H_{1q}^{\perp h}$. It is the chiral-odd transverse-spin dependent FF that describes the correlation of quark (q) transverse polarisation and hadron (h) transverse momentum. This mechanism leads to a left-right asymmetry in the distribution of hadrons produced in the fragmentation of transversely polarised quarks, which in SIDIS shows up as an azimuthal transverse spin asymmetry A_C (the "Collins asymmetry") in the distribution of produced hadrons. At leading order this asymmetry can be written as

$$A_C = \frac{\sum_q e_q^2 x h_1^q \otimes H_{1q}^{\perp}}{\sum_q e_q^2 x f_1^q \otimes D_{1q}} \qquad (2)$$

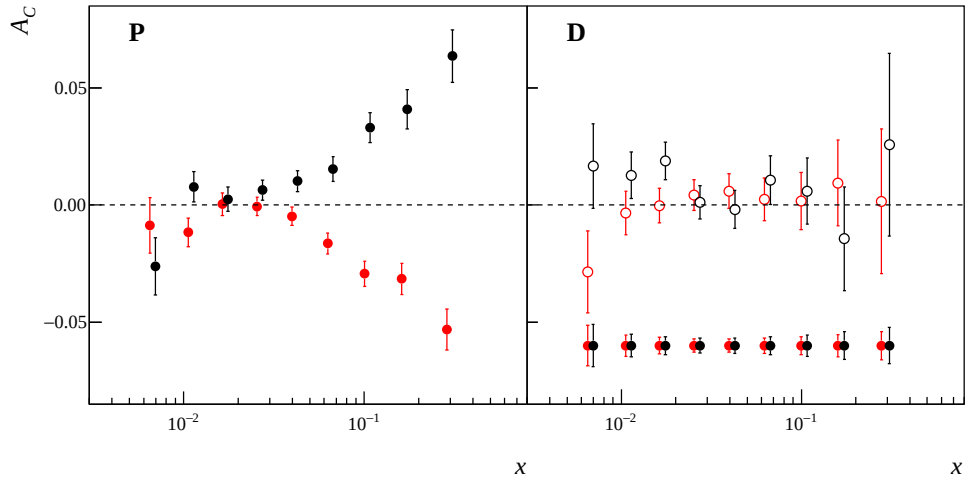

Figure 5: A_C obtained from the 2010 data with the polarised proton NH_3 target as a function of x (left plot) compared to the results we obtained [10] from the runs of 2002, 2003 and 2004 with polarised deuteron ^{6}LiD target (right plot). The red (black) points refer to positive (negative) hadrons. The full points at -0.06 in the right plot show the extrapolated statistical error from the proposed deuteron run.

where the sum is over all quark and antiquark flavours, D_q^h is the usual FF and $\otimes$ indicates the convolutions (different for numerator and denominator) over the intrinsic transverse momenta. The Collins effect shows up as a modulation $[1 + a_C \sin(\phi_h + \phi_S - \pi)]$ in the hadron azimuthal distribution. Here $\Phi_C = \phi_h + \phi_S - \pi$ is the Collins angle, and ϕ_h and ϕ_S are the azimuthal angles of the hadron transverse momentum $\boldsymbol{P}_{hT}$ and of the spin direction of the target nucleon with respect to the lepton scattering plane, in a reference system in which the z axis is the virtual-photon direction. The amplitude of the modulation is $a_C = D_{NN} f P A_C$, where D_{NN} is the transverse spin transfer coefficient from target quark to struck quark, f the dilution factor of the target material, and P is the proton (or deuteron) polarisation. In Fig. 5 the results [34] for A_C we have obtained from the 2010 data collected using as target NH_3, a polarised proton target, are shown as a function of x (left panel) and compared to the results we obtained [10] from the deuteron runs of 2002, 2003, and 2004, when as target we used ^{6}LiD (right panel).

It is clear that the accuracy of the data is considerably better for the proton target, in particular at large x, where the Collins asymmetry is large. In order to quantify this fact, it is instructive to look at the ratio of the errors, shown in Fig. 6 as a function of x. In order to understand this plot, one has to remember that, for small asymmetries, the statistical error is given by

$$\sigma_A \simeq \frac{1}{fP}\frac{1}{\sqrt{N}} = \frac{1}{FOM}\frac{1}{\sqrt{N}} \tag{3}$$

where N is the total number of hadrons and $FOM(= fP)$ is the figure of merit of the polarised target. Using $N_{d,h} = 15.5 \cdot 10^6$ and $N_{p,h} = 80 \cdot 10^6$ for the number of hadrons collected on p and d, and the known FOM values for the two targets, one gets

$$\frac{\sigma_{A_d}}{\sigma_{A_p}} = \frac{0.155 \cdot 0.80}{0.40 \cdot 0.50}\frac{\sqrt{80}}{\sqrt{15.5}} = 0.62 \cdot 2.3 = 1.4, \tag{4}$$

in the hypothesis that the spectrometer acceptance was the same for the proton and the deuteron runs. As a remark, it is interesting to note that in the ratio 4 the better FOM of

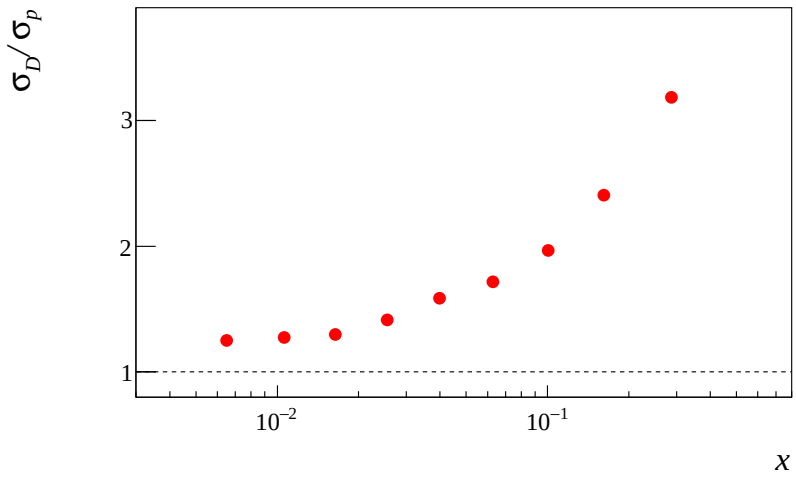

Figure 6: Ratio of the A_C statistical uncertainties on deuteron and proton as measured by COMPASS.

the deuteron target partly compensates the factor of 5 in statistics in favor of the proton target run. In Fig. 6, at small x, where statistics is largest, the ratio between the statistical uncertainties of the deuteron and the proton asymmetries is constant, an indication of the fact that the spectrometer acceptance was essentially the same at small x in the two data taking. The measured value of the ratio is 1.25, which indeed is close to the expected value of 1.4. The 10% difference is due to the fact that the polarised target cells diameter in the deuteron runs was 3 cm while for the proton runs it was 4 cm, which resulted in a 20% larger muon beam acceptance in the proton runs. Our plan is to run in 2021 with 4 cm target cells diameter as long as enough of the ^{6}LiD material will be available.

The most important information provided by Fig. 6 is however the dramatic increase of the ratio with x. This increase is due to the fact that there is a huge difference between the acceptance of the COMPASS P_T magnet utilized for the proton run and the SMC PT magnet in operation in 2002-2003-2004 for the measurements with the ^{6}LiD target. The COMPASS magnet has a polar acceptance of 180 mrad (as seen from the upstream end of the target) while the SMC magnet has a corresponding polar angle acceptance of 70 mrad. A reduced acceptance in scattering angle mainly translates into a reduced acceptance at large x-Bjorken, thus Fig. 6 essentially gives the square root of the ratio of the two acceptances as a function of x.

1.3.2 Projected errors after 1 year of deuteron run

Since target density and packing factors are essentially identical for ^{6}LiD and NH_3, it can be safely assumed that in one year of deuteron run in the conditions of the 2010 proton run $80{\cdot}10^6$ "good" hadrons will be collected, so that the errors on the new deuteron asymmetries will be equal to the present errors for the 2010 proton asymmetries scaled by the ratio of the FOM, namely they will be smaller by a factor of 0.62. The projected errors for the deuteron asymmetries are also plotted in Fig. 5, together with the existing results for the deuteron and proton asymmetries. We neglect the systematic errors which were estimated to be at most 0.5 times the statistical errors in the 2010 data.

Using the 2010 proton data and the projections of Fig. 5 for the statistical errors of the new deuteron data we have extracted the u- and d-quark transversity, in order to quantify the gain in statistical error in these fundamental PDFs. To carry through this evaluation

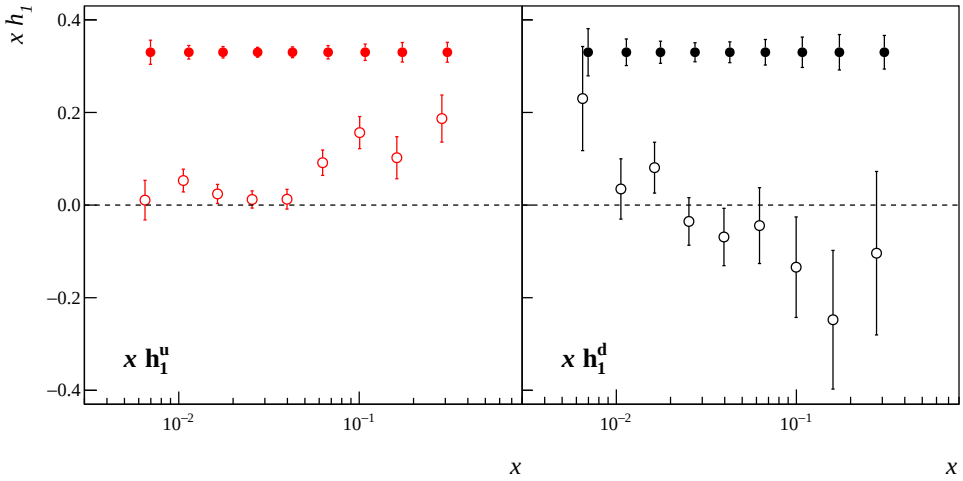

Figure 7: Values of u_v-quark (left) and d_v-quark (right) transversity extracted from the existing p and d data (open points), and the corresponding error bars estimated using the existing p data and the new d data (closed points).

we have followed the procedure of Ref. [13], for a point by point extraction of transversity directly from the measured SIDIS and $e^+e^- \to hadrons$ asymmetries.

The big advantage of this method is that

- it is simple, it avoids the use of parametrizations for the unknown functions, and the PDFs are calculated algebraically from the asymmetries

but

- it requires asymmetry measurements (p, d or n, identified final state particles) performed at the same x-values and in the same kinematic ranges.

This second point is the reason why we could not utilize all the available data (i.e. the HERMES measurements). A comparison between Fig. 1 and Fig. 3 however shows that the two procedures, i.e using the COMPASS data alone and the point-to-point extraction method, or doing a global analysis on all the existing data, give similar results. Therefore we leave the more complete and global approach to the specialized colleagues and present the result we obtained with the simplified analysis, which is already quite adequate to our purposes. The results are given in Fig. 7, which shows both the values of transversity (open points) extracted from the existing p and d data, and the corresponding error bars (closed points) estimated using the existing p data and the d data, with the projected errors of the new measurement. The impact of the proposed measurement is clearly quantified in Fig. 8, which gives the ratio, at each x value, of the present and projected errors on the extracted transversity PDFs. The gain in precision for the d-quark ranges from a factor of 2 at small x to a factor of 5 at large x, and is also important for the u-quark.

1.3.3 Projections for the tensor charge

In order to evaluate the impact of the proposed measurement on the statistical accuracy of the tensor charge one can introduce a functional dependence for h_1^q, to be fixed by fitting the point-to-point extracted values of $xh_1^{u_v}$ and $xh_1^{d_v}$ from the COMPASS data and then integrating the curves over the measured x-range. We neglect the Q^2 dependence of h_1 and take

$$xh_1^q(x) = a_q x^{b_q}(1-x)^{c_q}. \tag{5}$$

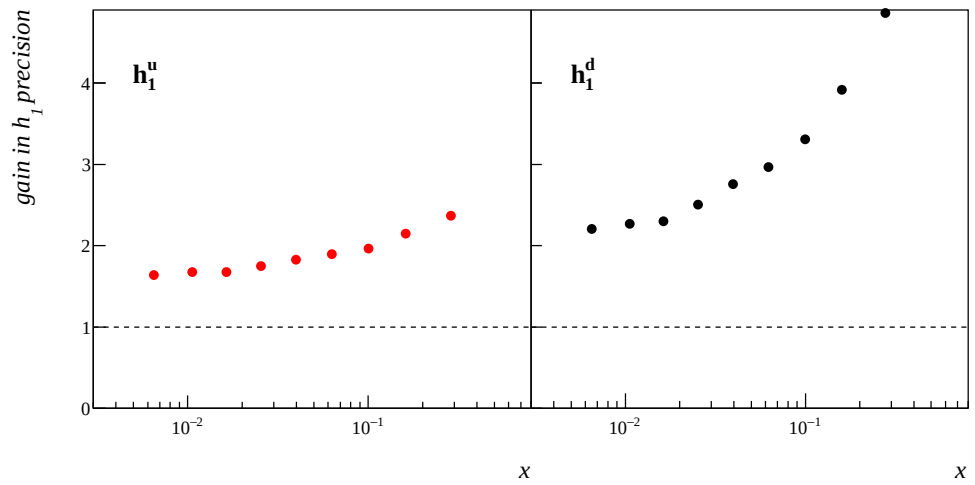

Figure 8: Ratio of the existing uncertainties on the extracted transversity and the projected uncertainties for u_v-quark (left) and d_v-quark (right).

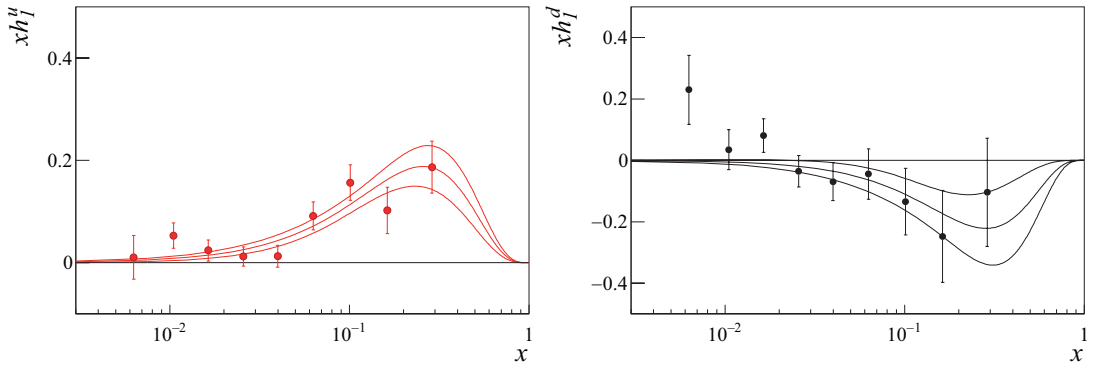

Figure 9: Extracted values of the valence quark transversity distributions $xh_1^{u_v}$ and $xh_1^{d_v}$ [13] with the curves from the fits with the 1σ uncertainty band indicated.

Unfortunately, the present statistical accuracy on xh_1^q with $q = u_v, d_v$ does not allow to safely determine all the parameters a_q, b_q and c_q and in particular their covariance matrix, needed for this exercise. We thus assumed $c_q = 4$, as suggested by the central values given by the fit. For the remaining two free parameters we get

$$a_{u_v} = 3.5 \pm 1.6,\ b_{u_v} = 1.3 \pm 0.2,\ ; a_{d_v} = -5.2 \pm 5.3,\ b_{d_v} = 1.5 \pm 0.5\,. \tag{6}$$

The comparisons between the fitted $xh_1^{u_v}$ and $xh_1^{d_v}$ and the extracted transversity values are shown in Fig. 9, together with the 68% uncertainty bands.

To estimate the impact of the proposed measurement on the extraction of the tensor charge, the curves have been numerically integrated in the range $0.003 < x < 0.21$. The integrated range excludes the last measured x bin, in order to not overlap with the future precise data from JLab12. The exercise has been done twice, the first time assigning to the quark transversity values the errors obtained from the extraction of Ref. [13], shown in Fig. 8, and a second time, reducing the errors by the estimated ratios as given in Fig. 7. Needless to say, the purpose of this exercise is not to give absolute values for the uncertainties on the extractions of the u- and d-quark tensor charges, but only to show the reduction in the statistical error obtained with the new run as compared to the present situation. The results are given in Table 1 together with the corresponding values

Table 1: Integrated values of h_1 and result for g_T from the fits with the present and the projected uncertainties.

	$0.003 < x < 0.21$		
errors	$\int dx h_1^{u_v}(x)$	$\int dx h_1^{d_v}(x)$	g_T
present	0.255 ± 0.043	-0.202 ± 0.112	0.45 ± 0.12
projected	0.211 ± 0.027	-0.212 ± 0.042	0.423 ± 0.050
	$0 < x < 1$		
present	0.59 ± 0.13	-0.61 ± 0.35	1.20 ± 0.37
projected	0.587 ± 0.077	-0.585 ± 0.119	1.172 ± 0.142

of $g_T = \int dx h_1^{u_v}(x) - \int dx h_1^{u_v}(x)$. In the range where we measure ($0.003 < x < 0.21$) the errors become a factor of 2.5 smaller. While the evaluation of the d-quark tensor charge presently has small statistical significance, the new measurement should provide an almost 5σ effect with respect to the presently estimated value, and the extraction of g_T in the x-interval in which COMPASS can measure has a small uncertainty. Only for completeness we have integrated the fitted functions also in the entire domain $0 < x < 1$, to give an idea of the contribution that COMPASS can give to the determination of the tensor charge. Again these estimates are meant only to propagate the statistical uncertainties from the measured PDF to the integrated tensor charges in order to evaluate the impact of the new data, and not to give a value for the tensor charge itself.

We are well aware that making use of a parametrizations for the transversity functions introduces a systematic uncertainty almost impossible to be estimated. This is a common problem with all global fits as clear from f.i. Ref. [**?**]. To avoid it, we have also estimated the quark tensor charges without any parametrization, integrating numerically the extracted transversity values, over the interval $0.003 < x < 0.13$, which corresponds to the first 7 values measured by COMPASS as a function of x. The data we will collect at $x > 0.13$ will be very important for a comparison with the future JLab data, both to assess compatibility and to investigate the Q^2 dependence. The data we will obtain in the range $0.003 < x < 0.13$ will on the contrary be unique, and they will allow an estimate of the value of the tensor charge in that range fully independent of any model. In this case the statistical errors become ± 0.027 for the u- tensor charge and ± 0.051 for the d- tensor charge, and ± 0.058 for g_T. If indeed SOLID will provide high accuracy measurements for $x > 0.1$ [35], so that the error on the integration in the range $0.13 < x < 1$ can be neglected with respect to the uncertainty of the integration in the COMPASS range, then the overall uncertainty on the tensor charge g_T will be the uncertainty of our future measurement.

To summarize, at large x, JLab will provide very accurate partial measurements for g_T. At smaller x ($0.003 < x < 0.1$) the COMPASS data will provide a contribution to g_T with an uncertainty of ± 0.06. Without the new deuteron data from COMPASS, the evaluation of the tensor charge from the future high precision JLab data would be affected by the error of the integration between 0 and 0.1 difficult to be ascertained, and the result will anyhow be model dependent. With the new COMPASS deuteron data, the uncertainty of the extrapolated contribution of the integration from 0 to 0.003 can reasonably be very small, and the uncertainty of the partial integration of the COMPASS data (± 0.06) will be the resulting uncertainty on the tensor charge g_T.

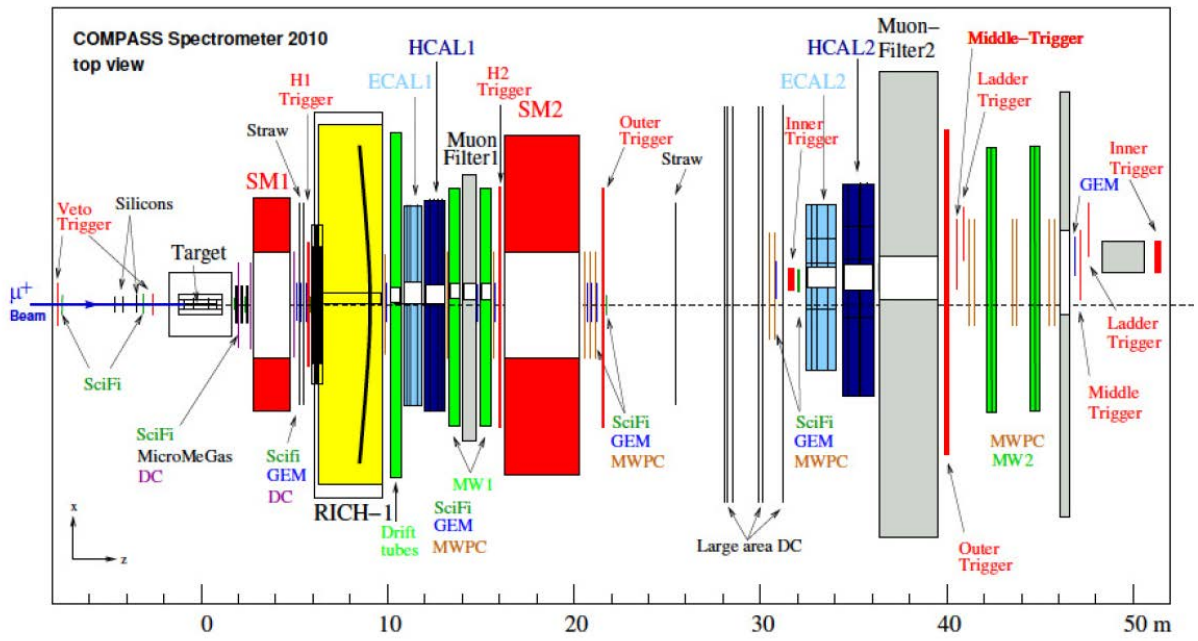

Figure 10: Schematic lay-out of the COMPASS spectrometer (top view) as it was used in 2010 and as it will be reassembled for the 2021 run.

1.4 Experimental Apparatus and Beam request

The apparatus to be used for the deuteron run is basically the COMPASS Spectrometer as it was used in the 2010 muon run, shown schematically in Fig. 10. This implies removing the absorber which will be used for the 2018 Drell-Yan run, moving the polarised target 2 m downstream to the position it had for the SIDIS runs, and reinstalling all the trackers and all the counters which were used in 2010. The polarised target will be housed in the large acceptance COMPASS PT magnet, and the target material will be the same which was used in the years 2002, 2003, 2004 and 2006, namely ^{6}LiD. For a better usage of the muon beam, the target cells diameter will be increased from 3 to 4 cm. The average polarisation of the target is expected to be the same as in the past deuteron runs ($\leq 50\%$).

The beam request is the same as for the 2010 proton run, namely 2.5×10^{13} protons delivered to the T6 target of the M2 beam line every 40.8 s. With an accelerator chain efficiency of 90% and a running time of 150 days a total of 6.1×10^{18} protons at T6 is expected. This number of protons is the basis of all the projections presented in this document, which are obtained from the number of reconstructed hadrons in the 2010 run.

The estimated uncertainties have been obtained assuming the COMPASS spectrometer availability and efficiency to be the same as in the 2010 run, but several upgrades have already been implemented over the past years and more upgrades are foreseen for running after 2020. Tracking will profit of the addition of several trackers over the past ten years, in particular the new large area DC5, the pixelized GEMs and Micromegas and several scintillating fiber hodoscopes. At variance with the past deuteron runs, electromagnetic calorimetry will also be available (ECAL1 and ECAL2). Here we consider unidentified hadrons only, but as in 2010, particle identification will be provided by the RICH1 detector, for which the completion of the upgrade done for the 2016 run is foreseen. In addition some increase in the collected data is expected from hardware upgrades of the last years,

in particular concerning the DAQ and trigger. Since no major upgrades of the present spectrometer are necessary for this measurement, it can start soon and take place in 2021.

1.5 Summary

We propose to improve our knowledge of the transverse spin structure of the nucleon by measuring 160 GeV muon semi inclusive DIS on a transversely polarised deuteron target. This measurement will complete the exploratory investigation of the transverse spin structure of the nucleon originally proposed by COMPASS 20 years ago. The measurement will be unique in the small x-Bjorken region, and complementary to corresponding measurements already approved at JLab. The proposed measurements will have a profound impact on the field, and their combination with the already taken proton data will allow to further clarify the properties of the up, down and sea quarks in the nucleon. Moreover, a combined analysis of the transversity measurement at CERN and at JLab will allow a determination of the isovector tensor charge with an accuracy of ± 0.06.

Quoting from our last proposal for a polarised SIDIS measurement [7], "the high intensity and polarisation of the muon beam together with the COMPASS polarised target and spectrometer make CERN a unique place to perform such measurement. This will not change until the construction of a high energy and luminosity polarised electron-ion collider in the longer term future".

1.6 TMD PDFs and SIDIS scattering (for ease of reference reproduced from [7], App. A)

The recent theoretical work on the nucleon structure points out the relevance of its transverse structure. A good knowledge of the transverse intrinsic momentum $\mathbf{k}_T$ carried by the partons and of its connection with the spin is needed to understand the parton orbital motion and to progress towards a more structured picture, beyond the collinear partonic representation.

In the QCD parton model, at leading twist, the nucleon structure is described by eight TMD PDFs: $f_1(x, \mathbf{k}_T^2)$, $g_{1L}(x, \mathbf{k}_T^2)$, $h_1(x, \mathbf{k}_T^2)$, $g_{1T}(x, \mathbf{k}_T^2)$, $h_{1T}^{\perp}(x, \mathbf{k}_T^2)$, $h_{1L}^{\perp}(x, \mathbf{k}_T^2)$, $h_1^{\perp}(x, \mathbf{k}_T^2)$ and $f_{1T}^{\perp}(x, \mathbf{k}_T^2)$, using the so-called Amsterdam notation. After integrating over $\mathbf{k}_T$ only the first three PDFs survive, yielding the number distribution $f_1(x)$ (or $q(x)$), the helicity distribution $g_1(x)$ (or $\Delta q(x)$), and the transversity distribution $h_1(x)$ (or $\Delta_T q(x)$ in the usual COMPASS notation). These three functions fully specify the quark structure of the nucleon at the twist-two level. Today, a lot of attention is put in particular on the TMD functions $f_{1T}^{\perp}$, the Sivers function which gives the correlation between the nucleon transverse spin and the quark intrinsic transverse momentum, $h_1^{\perp}$, the Boer–Mulders function which gives the correlation between the transverse spin and the intrinsic transverse momentum of a quark inside an unpolarised nucleon, and g_{1T}, which is the only chiral-even and T-even leading twist function in addition to f_1 and g_1.

A powerful method to access the poorly known TMD PDF is SIDIS on transversely polarised targets. In fact, on the basis of general principles of quantum field theory in the

one photon exchange approximation, the SIDIS cross-section in the COMPASS kinematic range can be written in a model independent way as:

$$\begin{aligned}
\frac{d\sigma}{dx\,dy\,dz\,d\phi_S\,d\phi_h\,dp_T^h} &= \frac{\alpha^2}{xyQ^2}\frac{y^2}{2(1-\epsilon)}\Big\{F_{UU} + \\
&+\sqrt{2\epsilon(1+\epsilon)}\cos\phi_h F_{UU}^{\cos\phi_h} + \epsilon\,\cos 2\phi_h\, F_{UU}^{\cos 2\phi_h} + \\
&+\lambda\sqrt{2\epsilon(1-\epsilon)}\sin\phi_h F_{LU}^{\sin\phi_h} + \\
&+S_L\Big[\sqrt{2\epsilon(1+\epsilon)}\sin\phi_h F_{UL}^{\sin\phi_h} + \epsilon\sin 2\phi_h F_{UL}^{\sin 2\phi_h} + \\
&\quad + \lambda\left(\sqrt{1-\epsilon^2}F_{LL} + \sqrt{2\epsilon(1-\epsilon)}\cos\phi_h F_{LL}^{\cos\phi_h}\right)\Big] + \\
&+S_T\Big[\sin(\phi_h-\phi_S)F_{UT}^{\sin(\phi_h-\phi_S)} + \epsilon\sin(\phi_h+\phi_S)F_{UT}^{\sin(\phi_h+\phi_S)} + \\
&\quad + \epsilon\sin(3\phi_h-\phi_S)F_{UT}^{\sin(3\phi_h-\phi_S)} + \\
&\quad + \sqrt{2\epsilon(1+\epsilon)}\sin\phi_S F_{UT}^{\sin\phi_S} + \\
&\quad + \sqrt{2\epsilon(1+\epsilon)}\sin(2\phi_h-\phi_S)F_{UT}^{\sin(2\phi_h-\phi_S)} \\
&\quad + \lambda\Big(\sqrt{1-\epsilon^2}\cos(\phi_h-\phi_S)F_{LT}^{\cos(\phi_h-\phi_S)} \\
&\qquad + \sqrt{2\epsilon(1-\epsilon)}\cos\phi_S F_{LT}^{\cos\phi_S} \\
&\qquad + \sqrt{2\epsilon(1-\epsilon)}\cos(2\phi_h-\phi_S)F_{LT}^{\cos(2\phi_h-\phi_S)}\Big)\Big]\Big\}. \quad (7)
\end{aligned}$$

Here ϕ_S and ϕ_h are the azimuthal angles of the nucleon transverse spin and of the hadron transverse momentum $\boldsymbol{p}_T^h$ in the Gamma–Nucleon System, α is the fine structure constant, λ is the lepton helicity, S_T and S_L are the nucleon transverse and longitudinal polarisation. Neglecting the terms in $\gamma^2 = (2Mx/Q)^2$, the quantity ϵ is given by $\epsilon = (1-y)/(1-y+y^2/2)$.

The r.h.s. structure functions F's in general depend on Q^2, x, z and p_T^h. Their superscripts refer to the corresponding azimuthal asymmetries. The subscripts refer to the beam and to the target polarisation (U means unpolarised, L longitudinally polarised, and T transversely polarised). Since the modulations which appear in the cross-section for unpolarised, longitudinally polarised and transversely polarised nucleons are independent combinations of the azimuthal angles, all of them can be measured using data taken with unpolarised, longitudinally polarised and transversely polarised targets.

In the S_T-dependent part of the cross-section, only four of the eight structure functions are of leading order. They are:

- $F_{UT}^{\sin(\phi_h+\phi_S)} \propto h_1 \otimes H_1^\perp$, where h_1 is the transversity distribution, $H_1^\perp$ is the Collins fragmentation function and $\otimes$ indicates the convolution over the quark intrinsic transverse momentum summed over the quark flavours. When divided by F_{UU} it is the Collins asymmetry measured by COMPASS and HERMES;
- $F_{UT}^{\sin(\phi_h-\phi_S)} \propto f_{1T}^\perp \otimes D$, where $f_{1T}^\perp$ is the Sivers function and D is the unpolarised fragmentation function. When divided by F_{UU} it is the Sivers asymmetry measured by COMPASS and HERMES;
- $F_{UT}^{\sin(3\phi_h-\phi_S)} \propto h_{1T}^\perp \otimes H_1^\perp$, and
- $F_{LT}^{\cos(\phi_h-\phi_S)} \propto g_{1T} \otimes D$.

A complete list of the TMD PDFs which appear in all the structure functions can be found e.g. in Ref. [6]

2 Determination of the proton radius using high-energy μp scattering

2.1 Electromagnetic form factors and radii of the proton

The physics of the proton as the charged nuclear building block of matter is at the core of interest in the quest for understanding nature. As consequence of its inner structure, the electromagnetic form factors G_E and G_M encode the response of the proton to outer electric and magnetic fields, respectively. As worked out in the following chapter, the squares G_E^2 and G_M^2 can be measured in non-polarized elastic lepton scattering off the proton, which has been done extensively since the 1950's with the pioneering work of R. Hofstadter [36]. The gross feature of the form factors is a dependence on the squared momentum transfer Q^2 given by

$$G_E(Q^2) = G_M(Q^2)/\mu_p = \frac{1}{(1+Q^2/a^2)^2} \tag{8}$$

called the dipole approximation, which can be motivated by a substructure of the proton consisting of three constituent quarks. The constant a has been determined in electron scattering to be about $a^2 \approx 0.71\,\mathrm{GeV}^2/c^2$. The functional behavior with $a^2 = 0.71\,\mathrm{GeV}^2/c^2$ is used as the standard reference dipole form $G_D(Q^2)$.

The respective charge and magnetic moment distributions in space are obtained by Fourier transformation of the form factors, and specifically the electric mean-square charge radius is related to form factor by

$$\langle r_E^2 \rangle = -6\hbar^2 \left.\frac{dG_E(Q^2)}{dQ^2}\right|_{Q^2\to 0} \overset{dipole}{=} \frac{12}{a^2} \approx (0.81\mathrm{fm})^2 \tag{9}$$

More refined fits to the measured shape of the form factors are often given as polynomials or other analytic functions of Q^2 multiplying the dipole approximation of Eq. 8. The so far most elaborate measurement of the proton form factors by elastic electron scattering have been carried out at the Mainz university accelerator MAMI [37, 38], and a parameterization of the results at small values $Q^2 < 0.2\,\mathrm{GeV}^2/c^2$ is shown in the upper plot of Fig. 11. Compared to earlier electron scattering data, the G_M^2 shows a positive deviation with respect to G_D^2, while G_E^2 starts with a steeper slope, corresponding to a charge radius, with the systematic uncertainties summed up linearly, $r_E^{rms}=\sqrt{\langle r_E^2\rangle}=(0.879\pm0.011)\,\mathrm{fm}$. It is at variance with the value found in laser spectroscopy of muonic hydrogen, $r_{E,\mu H}^{rms}=(0.841\pm0.001)\,\mathrm{fm}$ [39, 40], and this discrepancy of more than three standard deviations triggered many efforts to clarify its origin [41, 42, 43, 44, 45, 46, 47].

2.2 Experiments targeting the proton radius puzzle: the COMPASS case

The COMPASS collaboration proposes here to measure **elastic muon-proton scattering** with a high-energetic muon beam on a hydrogen gas target over a momentum transfer range particularly sensitive to the proton charge radius. This means, on the one hand, to measure the cross-section to come as close as possible to Q^2=0 as required by Eg. 9, and on the other hand, to cover a sufficient range in momentum transfer in order to constrain the slope of the cross-section on the desired level of precision. As illustrated in Fig. 11, this range is approximately $0.001 < Q^2/(\mathrm{GeV}^2/c^2) < 0.02$: At smaller values of Q^2, the deviation from a point-like proton is on the 10^{-3} level and thus smaller than unavoidable systematic effects, as the variation of the detector efficiencies with Q^2 that can not be controlled more accurately with the currently available methods. At higher

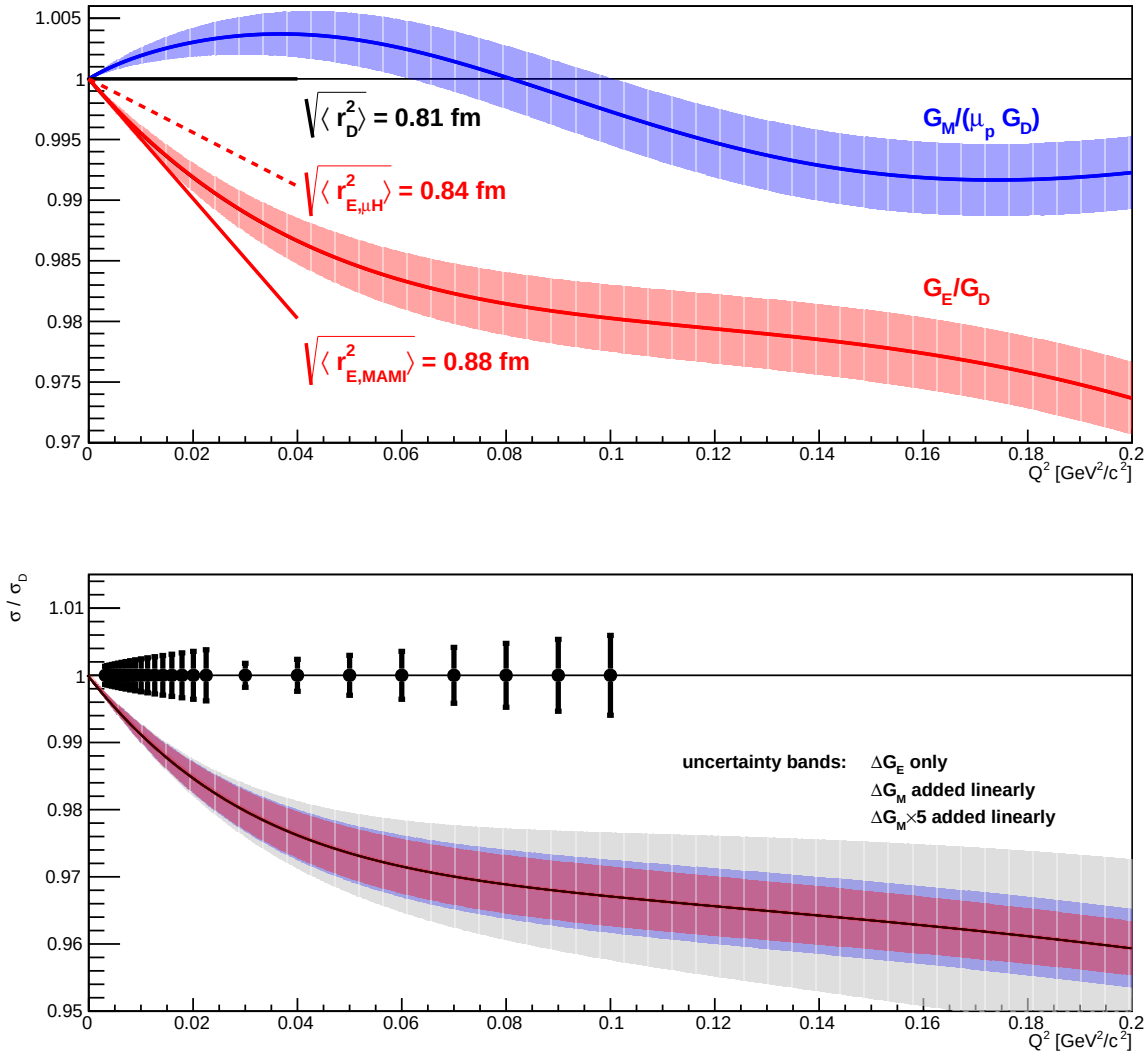

Figure 11: Upper plot: proton form factors G_E and G_M as measured at MAMI, presented relative to the dipole form G_D as given in the text. Lower plot: corresponding cross-section behavior, relative to the standard dipole form. The innermost uncertainty band corresponds to the effect of the uncertainty of G_E only, while for the (blue) middle band the uncertainty from G_M has been added linearly, and for the outer (gray) band the contribution from ΔG_M has been increased by a factor of five. The dots with error bars, arbitarily placed at 1, represent the achievable statistical precision of the proposed measurement, down to Q^2=0.003 GeV$^2/c^2$, where the statistical uncertainties are expected to dominate the systematic point-to-point uncertainty. There will be data from the proposed experiment down to $Q^2 \leq$0.001, with the statistical uncertainty further shrinking according to the increasing cross-section with $Q^2 \to 0$, *cf.* Eq. 10, which are omitted here for conciseness. For a discussion of the uncertainty contributions at different Q^2 regions, see the text.

$Q^2 > 0.02\mathrm{GeV}^2/c^2$, the non-linearity of the Q^2 dependence becomes the predominant source of uncertainty, and can not be used to determine the proton radius, unless more elaborate theory input is assumed.

For reaching the small momentum transfers, it is relevant to observe the recoil protons. Due to their small energy, this implies the target to be the detector volume at the same time. This can be realized by a Time Projection Chamber (TPC) operated with pure hydrogen gas. Such a target has been developed by PNPI [48, 49] and is in the testing phase for an analogous experiment using electron scattering at Mainz.

Several experiments are currently ongoing or proposed for refining the knowledge on **electron-proton** elastic scattering [41, 42, 50, 51]. This includes the mentioned TPC experiment at MAMI [50], but also the inital-state radiation experiment of the A1 collaboration [51]. All experiments of electron scattering are challenged by the required QED radiative corrections, which are as large as 20% due to the small electron mass. Currently, it is unclear how the precision of those corrections can be controlled on the desired below-1% level. Hence, independent of the outcome of any measurements done with electrons, those with muons will test systematic effects related to radiative corrections, since they are substantially smaller for muons due to their much larger mass.

Despite this obvious benefit, there are still significant systematic effects expected for measurements for **muon-proton** elastic scattering at **low muon beam energies**, *e.g.* discussed for the proposed MUSE experiment [45]. Apart from corrections for the pion component in the beam and muon decays, there is a substantial correction for the Coulomb distortion of the low-velocity muon wave function. The latter is estimated to be on the level of one percent for larger scattering angles, however with an unclear relation to the other radiative corrections, which introduces a systematic uncertainty for which an experimental test is most convincing. Such a test is best realized with scattering at very high energies, where the Feshbach correction reduces to a negligible level.

The highest precision on the proton radius is claimed by the the investigation of atomic level splittings [39, 40, 43, 44] that are very accurately measured by laser spectroscopy. From 1S transitions in **muonic hydrogen**, the above-mentioned value 0.841 fm has been determined, by correcting the measured frequency for all known QED effects and attributing the remaining effect to the proton finite size. By starting with the measurement of the single number, this approach is clearly less detailed than a measurement of the form factor behaviour over an extended range in Q^2, which allows for checking *e.g.* the assumption made for the linear behaviour of the form factor in the studied Q^2 range.

In summary, the proposed muon-proton scattering using a high-energy muon beam for the determination of the proton radius we regard as an important and unique cornerstone in the quest for solving the proton radius puzzle. It is seen very timely in view of the highly competitive and dynamic ongoing research in the field, to realize the measurement at COMPASS as soon as the scheduling and the required preparatory steps allow.

2.3 Elastic lepton-proton scattering

The cross-section for elastic muon-proton scattering to first order is

$$\frac{d\sigma}{dQ^2} = \frac{\pi\alpha^2}{Q^4\, m_p^2\, \boldsymbol{p}_\mu^2} \cdot \left[\left(G_E^2 + \tau G_M^2\right) \frac{4E_\mu^2 m_p^2 - Q^2(s - m_\mu^2)}{1+\tau} - G_M^2 \frac{2m_\mu^2 Q^2 - Q^4}{2} \right] \tag{10}$$

where $Q^2 = -t = -(p_\mu - p_{\mu'})^2$, $\tau = Q^2/(4m_p^2)$ and $s = (p_\mu + p_p)^2$. The squared centre-of-momentum energy s is given, in the laboratory system, by $s = 2E_\mu m_p + m_p^2 + m_\mu^2$ with E_μ

the energy, and $\boldsymbol{p}_\mu$ the three-momentum of the incoming muon colliding with a proton at rest.

The different dependence on the beam energy E_μ of the two terms in Eq. 10 that are proportional to G_M^2 allows, in principle, for the "Rosenbluth separation" of the two form factor contributions G_E^2 and G_M^2, by measuring the cross-section at constant Q^2 and, at least, two different beam energies (or correspondingly at different muon scattering angles). For small $Q^2 < m_\mu^2$, the relative contribution of the second term is approximately m_μ^2/E_μ^2, and for beam energies $E_\mu > 50\,\mathrm{GeV}$ it is an effect of less than 10^{-5}, which is unmeasurably small and thus can be neglected.

Consequently, with the proposed high-energy muon beam, one effectively determines the combination $(G_E+\tau G_M)$, and at small Q^2 (*i.e.* small τ) this amounts to a measurement of G_E when the small expected contribution from G_M is corrected for. Even with a conservative estimate of the uncertainty from G_M, a factor of five larger than the one claimed in the MAMI analysis, the uncertainty on G_E and thus on the charge radius stay well below 0.1%.

2.4 Measurement at COMPASS

We propose to measure elastic muon-proton scattering employing a 100 GeV muon beam on a pressurized hydrogen gas target. For the core of the measurement aiming at a precise measurement of the proton radius, the relevant momentum transfers $0.001 < Q^2/(\mathrm{GeV}^2/c^2) < 0.02$ are measured by operating the target as a TPC for detecting the proton recoil tracks. The pressure of the gas is optimized for having on the one hand sufficiently low stopping power such that the proton recoil tracks are detectable, and on the other hand they still fit in the TPC volume. The pressure ranges from 4 to 20 bar. The respective gas system has been developed and is in the test phase at MAMI. The details of the readout are to be adapted to the COMPASS environment and are currently under study. For higher recoil energies and thus the possibility to access a broader range of the form factor evolution in Q^2 a similar hydrogen cell is envisaged, with a cylindric array of scintillating fiber (SciFi) rings surrounding the interaction region.

The muon scattering kinematics are measured with the COMPASS spectrometer in its standard muon setup. To allow for the detection of the elastic, *i.e.* almost unscattered, tracks the beam killer components are excluded from the trigger. The central parts of the tracking detectors are activated, and the silicon telescopes surrounding the TPC are used for measuring with high accuracy the muon scattering angle. In addition, the electromagnetic calorimeters serve to control the (rare) radiative events.

Since triggering solely on the proton recoil implies Q^2-dependent efficiency variations that can not be controlled from the data themselves, a trigger component from the muon trajectory is foreseen. The beam rate is too high to record all events. Therefore, the beam trigger is extended by a new component that allows to veto muons with a scattering angle below about 5μrad. This suppresses muons that have experienced multiple (small-angle) scattering only, which amounts to 99% of the incoming muons. In contrast muons are efficiently selected with a scattering angle in the target larger than 100μrad, corresponding to momentum transfers larger than $10^{-4}\,\mathrm{GeV}^2/c^2$. A scenario could be realized with SciFi components surrounding the silicon detectors, however solutions with thinner detectors, such as silicon pixel detectors with a readout sufficiently fast for the trigger would be desirable for minimizing the multiple scattering as a source of systematic uncertainty. The respective topological trigger component is referred to as "kink trigger" in Tab. 2. For the longer-range future, COMPASS aims at a triggerless readout, which can solve

current issues of rate capability and allows for realizing the described event selection in an elegant and efficient manner for the proposed measurement.

For the higher-Q^2 region, the full beam rate has to be used, in order to compensate for the $1/Q^4$ behaviour of the Mott cross-section. Then, however, it is easier to realize a fully efficient trigger on the recoil protons that are stopped in the SciFi rings of the additional target setup mentioned above.

Since the TPC is tested to operate at a beam rate of $2 \cdot 10^6$/s, the proposal is currently based on this intensity, which is however a factor of 25 below the full available muon beam intensity. In that regard, the very different beam profile at COMPASS compared to the MAMI electron "pencil" beam, the muon having a broad diameter of ~ 20 mm, can be used for dissolving ambiguities in associating muon and proton signals. For the purpose, the new readout structure is foreseen to be sufficiently fine segmented in the range of $1 \times 1\,\mathrm{mm}^2$.

The respective conservative estimates for the beam time in 2022 are given in Tab. 2, assuming two pressure sets for the TPC at 4 and 20 bar, in order to cover the relevant Q^2 range, and 20 days of running for the higher-Q^2 region.

Table 2: COMPASS μ-beam parameters and typical numbers used to estimate total count rates and accuracies. We assume a maximum trigger rate of 100 kHz. We apply scaling by a factor 14 to convert the maximum beam intensity to a time-averaged intensity including duty cycles, SPS and COMPASS efficiencies, as derived from experience. Numbers denoted by (*) are used to derive the integrated luminosities.

beam energy	100 GeV
muons per spill (max)	$2.7 \cdot 10^8\,\mu$/spill
spill length	4.8 s
mean duty cycle	18%
spills per minute	3.3
efficiency of SPS	0.8
DAQ, veto dead times*	0.5
instantaneous intensity μ/s	$5 \cdot 10^7\,\mu$/s
effective maximum beam rate	$4 \cdot 10^6\,\mu$/s
mean effective intensity* μ/min (max)	$2.4 \cdot 10^8\,\mu$/min
instantaneous intensity μ/s (kink trigger)	$2 \cdot 10^6\,\mu$/s
mean effective intensity* μ/min (kink trigger)	$1.2 \cdot 10^7\,\mu$/min
beam spot size	8×8 mm^2
beam divergence	1 mrad
total days of beam time*	180
beam time for each TPC pressure setting*	80
beam time for SciFi recoil detection*	20
target length H_2 target*	60 cm
integrated luminosity H_2 @ 4bar	$8.9 \cdot 10^6$/mb
integrated luminosity H_2 @ 20bar	$4.45 \cdot 10^7$/mb

The statistical uncertainties that can be achieved in the sketched experiment are shown in Fig. 11 in a suitable segmentation of the data in Q^2 bins. The data set is sufficient to constrain the proton radius to better than 0.01 fm precision.

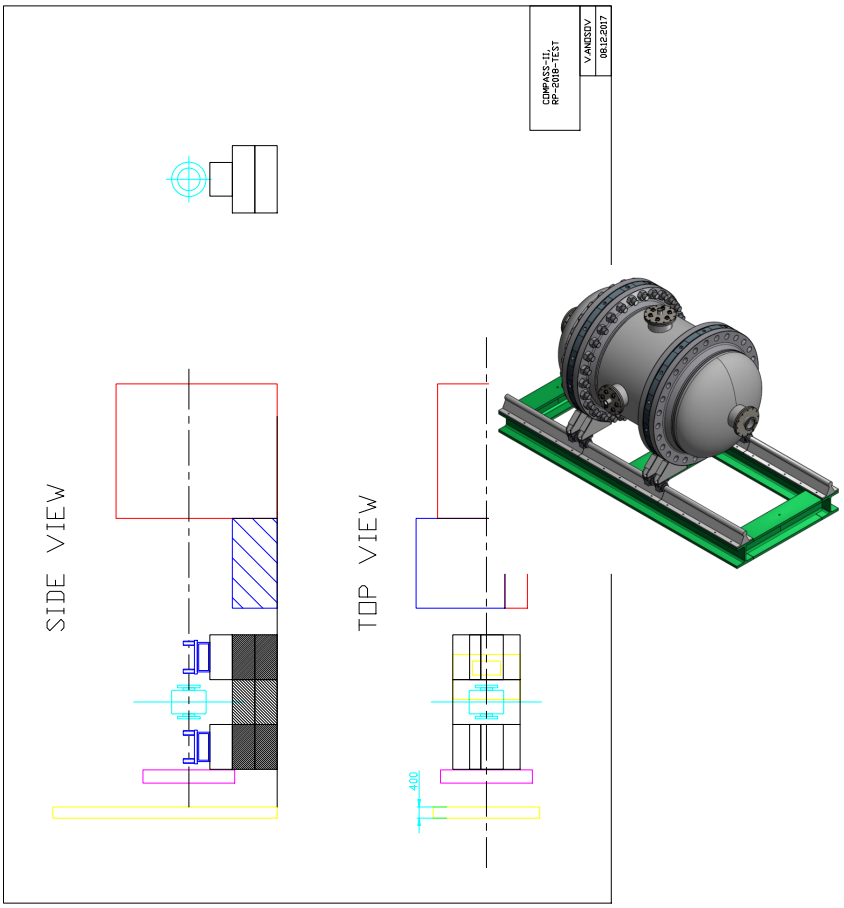

Figure 12: Drawing of the setup for the proposed test in EHN2 during the 2018 beam time. The active-target TPC, also shown in the insert, will be sandwiched between silicon telescopes.

2.5 Test Measurement at COMPASS in 2018 and 2021

For a successful running in 2022, it is indispenable to perform test measurements beforehand, and test the various components for their readiness for the experiment.

The biggest challenge of the modified setup is the integration of the new TPC, that currently follows a different readout scheme not fitting the COMPASS electronics. Adaptions on both sides are foreseen, and will take about two years of development, including a new readout plane for the TPC. The principle of the measurement, specifically the observation of recoils in the TPC in coincidence with muon tracks measured by a silicon telescope, can however be shown already in a test beam phase in 2018. The full setup is foreseen to be tested along the COMPASS beam time in 2021, including the new trigger. Several options for integration of the TPC setup in the main setup for SIDIS on a transversely polarized deuteron target are to be discussed.

The proposed setup for the test measurement in 2018 is foreseen at the test bench downstream of the COMPASS experiment and sketched in Fig. 12. Two silicon telescopes are foreseen to surround the TPC, in order to determine the incoming and the scattered muon trajectory, respectively. Their readout is triggered by a scintillation counter placed

in front. The muon component of the pion beam, which will be used in this test, can be assumed to be sufficiently small, such that all beam triggers can be read out.

Issues to be investigated in the test measurement in 2018 include:

- How does the TPC operate in the muon beam, which is much wider than the pencil beam at MAMI? How should the future readout structure be optimally segmented and equipped with electronics?
- Can the expected separation of the muon kinematics in scattered and unscattered characeristics, as planned to be used in the described kink trigger, be achieved?

The setup is planned to be prepared before the running of the experiment, such that measurements with about two weeks of beam can be performed during the first three weeks of the 2018 beam time.

– HARDWARE –

3 Experimental requirements

The apparatus needed for the transverse deuteron run is essentially the present one, with some detector components refurbished or upgraded as detailed in Table 3. The apparatus requirements imposed by the new measurement, namely the proton radius, are rather modest, but do require additional detectors. Apart the target proton recoil detectors, the determination of the muon scattering is vital and we have to refurbish at least one silicon station. In addition, we need longer optical benches to achieve internal stability for both silicon telescopes and minimise thermal displacements. The installation of new detectors also imposes requirements on new electronics and their implementation into the COMPASS DAQ scheme.

Detector	Responsibility	new/existing
μ Beam	CERN	existing
electron Beam	CERN	new
BMS	Bonn HISKP	existing
Luminosity measurement	Freiburg, Mainz	upgrade
polarised target	Yamagata, Bochum, Czech G., Dubna	existing
Silicon telescopes	TUM	existing
Silicon station	TUM	new
TPC and pressure tank	Gatchina	new
TPC gas system	Gatchina	new
TPC RO	Gatchina, Bonn HISKP, Freiburg, Saclay	new
SciFi target	TUM	new
SciFi tracker	Bonn HISKP	existing
SciFi TDC	Freiburg	new
GEM	Bonn HISKP, TUM	refurbish
Micromegas	Saclay	existing
Straws	Illinios, Czech Group	existing
MWPC	Torino	upgrade
DC	Saclay, Illinios, Taipei	existing
RICH	Trieste, Calcutta, Czech Group	upgrade
RICHWALL	Torino	existing
HCAL1	Dubna	existing
HCAL2	Protvino	existing
ECAL1	Protvino	existing
ECAL2	Protvino	existing
MW1	Dubna	existing
MW2	Protvino	existing
W45	CERN	existing
DAQ	TUM, Czech Group	existing
Trigger	Bonn PI, Mainz	existing
TPC Trigger	TUM, Mainz	new
Slow control	Lisbon	upgrade
Infrastructure	CERN	existing

Table 3: Planned requirements and responsibilities for equipment

Acknowledgements

The authors thank J. Bernhard, M. O. Distler, N. Kaiser for useful advice and comments, critical reading, and/or technical help.

References

[1] P. J. Mulders et al., Nucl. Phys. B461 (1996) 197, [Erratum: Nucl. Phys. B484, 538 (1997)] We use the "Amsterdam notation" as in this publication.
[2] V. Barone et al., Prog. Part. Nucl. Phys. 65 (2010) 267.
[3] C. A. Aidala et al., Rev. Mod. Phys. 85 (2013) 655.
[4] H. Avakian et al., Eur. Phys. J. A52 (6) (2016) 150, [Erratum: Eur. Phys. J. A52 No.6 (2016) 165].
[5] A. Kotzinian, Nucl. Phys. B441 (1995) 234.
[6] A. Bacchetta et al., JHEP 02 (2007) 093.
[7] COMPASS, Collaboration, Addendum 2 to the COMPASS Proposal, CERN-SPSC-2009-025 SPSC-M-769, SPSLC-P-297 Add.2 (2009).
[8] D. W. Sivers, Phys. Rev. D41 (1990) 83.
[9] J. C. Collins, Nucl. Phys. B396 (1993) 161.
[10] COMPASS, E. S. Ageev et al., Nucl. Phys. B765 (2007) 31.
[11] Jefferson Lab Hall A, X. Qian et al., Phys. Rev. Lett. 107 (2011) 072003.
[12] Jefferson Lab Hall A, Y. X. Zhao et al., Phys. Rev. C90 (5) (2014) 055201.
[13] A. Martin et al., Phys. Rev. D91 (1) (2015) 014034.
[14] A. Martin et al., Phys. Rev. D95 (9) (2017) 094024.
[15] M. Anselmino et al., Phys. Rev. D87 (2013) 094019.
[16] M. Anselmino et al., Phys. Rev. D86 (2012) 014028.
[17] Z.-B. Kang et al., Phys. Rev. D 93 (2016) 014009, https://link.aps.org/doi/10.1103/PhysRevD.93.014009.
[18] M. Anselmino et al., Phys. Rev. D 92 (2015) 114023, https://link.aps.org/doi/10.1103/PhysRevD.92.114023.
[19] M. Radici et al., JHEP 05 (2015) 123.
[20] COMPASS, C. Adolph et al., Phys. Lett. B736 (2014) 124.
[21] COMPASS, C. Adolph et al., Phys. Lett. B753 (2016) 406.
[22] X. Artru et al., Z. Phys. C73 (1997) 527.
[23] X. Artru, Prob. Atomic Sci. Technol. 2012N1 (2012) 173.
[24] COMPASS, C. Adolph et al., Phys. Lett. B772 (2017) 854.
[25] J. Matouek, Few Body Syst. 58 (3) (2017) 126.
[26] B. Parsamyan, Int. J. Mod. Phys. Conf. Ser. 40 (2016) 1660029.
[27] COMPASS, C. Adolph et al., Nucl. Phys. B865 (2012) 1.
[28] COMPASS, C. Adolph et al., Phys. Lett. B731 (2014) 19.
[29] J.-W. Chen et al., Nucl. Phys. B911 (2016) 246.
[30] T. Bhattacharya et al., Phys. Rev. D94 (5) (2016) 054508.
[31] A. Courtoy et al., Phys. Rev. Lett. 115 (2015) 162001.
[32] JLab, Hall-A Proposal E12-10-006, SIDIS with Transversely Polarized 3He Target using SoLID (2009), http://hallaweb.jlab.org/collab/PAC/PAC35/PR-10-006-SoLID-Transversity.pdf.
[33] JLab, Hall-A Proposal E12-11-108, SIDIS with Polarized Proton Target using SoLID (2011), https://www.jlab.org/exp_prog/proposals/11/PR12-11-108.pdf.
[34] COMPASS, C. Adolph et al., Phys. Lett. B717 (2012) 376.

[35] Z. Ye et al., Phys. Lett. B767 (2017) 91.
[36] R. Hofstadter et al., Phys. Rev. 98 (1955) 217.
[37] A1 Collaboration, J. C. Bernauer et al., Phys. Rev. Lett. 105 (2010) 242001, https://link.aps.org/doi/10.1103/PhysRevLett.105.242001.
[38] J. C. Bernauer, J. Phys. Conf. Ser. 381 (2012) 012006.
[39] R. Pohl et al., Nature 466 (2010) 213.
[40] CREMA, R. Pohl, Hyperfine Interact. 227 (1-3) (2014) 23.
[41] A. Antognini et al., EPJ Web Conf. 113 (2016) 01006.
[42] PRad, A. H. Gasparian, JPS Conf. Proc. 13 (2017) 020052.
[43] R. Pohl et al., Metrologia 54 (2017) L1.
[44] CREMA collaboration, F. Biraben et al., Proposal for an experiment at PSI: Lamb shift in muonic helium, https://www.ethz.ch/content/dam/ethz/special-interest/phys/particle-physics/precisionphysicsatlowenergy-dam/Research/Proposal_muHe_pdf.pdf.
[45] MUSE, R. Gilman et al., arXiv:1303.2160.
[46] OLYMPUS, B. S. Henderson et al., Phys. Rev. Lett. 118 (9) (2017) 092501.
[47] T. Suda, Electron scattering experiment off proton at ultra-low q^2 (2016), http://www2.yukawa.kyoto-u.ac.jp/~min2016/slides/Suda_MIN2016.pdf, talkpresentedatMesoninNucleusconference.
[48] A. A. Vorobyov et al., Nucl. Instrum. Meth. 119 (1974) 509.
[49] S. Ilieva et al., Nucl. Phys. A875 (2012) 8.
[50] A. Vorobyov, Proton radius status and perspective, incl.: Proposal for high precision measuremens of the *ep* differential cross sections at small t values with the recoiled proton detector (2016), https://indico.cern.ch/event/544849/contributions/2213665/attachments/1301151/1942517/Vorobyev_ep_report_27_june_2016.pdf.
[51] M. Mihovilovi et al., Phys. Lett. B771 (2017) 194.